Electron–relaxation-mode interaction in $BaTiO_3$:Nb

M. Maglione and M. Belkaoumi
Laboratoire de Physique du Solide, Université de Bourgogne, Boîte Postale 138, F-21004 Dijon CEDEX, France
(Received 1 April 1991)

Dielectric relaxation was previously reported in $BaTiO_3$ and $BaTiO_3$:Fe single crystals at radio frequencies [M. Maglione *et al.*, Phys. Rev. B **40**, 11 441 (1989)]. We have measured the dielectric dispersion in four $BaTiO_3$:Nb samples ($x_{Nb} < 0.3$ at. %) as a function of frequency ($10 < f < 10^9$ Hz) and temperature ($20 < T < 450$ K). The electronic conductivity of $BaTiO_3$:Nb enhances drastically the relaxation step at all temperatures. In the rhombohedral phase of $BaTiO_3$:Nb ($T < 180$ K), an unusual slowing down of the relaxation motion is measured. The relaxation time increases to more than 10^{-2} s at 20 K while the relaxation step is temperature independent. The precursor effect of this slowing down is a maximum in the dc conductivity. A simple electron–relaxation-mode coupling model may explain such behavior.

I. INTRODUCTION

After a wealth of experimental results, the exact nature of the phase transition in barium titanate ($BaTiO_3$) is still a matter of debate in the recent literature.

In the 1960s, the displacive picture was used to describe the whole set of experimental results.[1] In this model, the long-wavelength oscillations of the Ti^{4+} ions against their oxygen cage result in a dielectric divergence at the phase transition temperature T_c. Thus, the mode softening and the dielectric properties were well connected to the lattice symmetry. This model was first questioned in the early 1970s on the basis of x-ray-diffuse-scattering experiments in $BaTiO_3$ and its isomorph ($KNbO_3$) (potassium niobate).[2] In the high-temperature cubic phase of both crystals, diffuse stripes were explained in terms of localized lattice distortion arising from the noncubic displacement of Ti^{4+} (Nb^{5+} for $KNbO_3$) ions along the ⟨111⟩ directions. These ⟨111⟩ off-center distortions were correlated along ⟨100⟩ chains of some 100 Å length. During the past ten years, continuous improvement of both crystal quality and experimental devices has led to additional experimental investigation.

The breaking of pure soft-phonon dynamics in $KNbO_3$ and $BaTiO_3$ was evidenced by infrared-reflectivity[3] and Raman-scattering[4,5] experiments.

Electron paramagnetic resonance probed the dynamics of the local distortions in $BaTiO_3$.[6] Relaxation times longer than 10^{-10} s were found in $BaTiO_3$:Fe,Cr,Mn.

The correlation lengths of these local distortions are hardly derived from magnetic-resonance data. However, a systematic NMR investigation of the ^{181}Ta relaxation was performed in $KTa_{1-x}Nb_xO_3$ as a function of x. The main result of this work[7] is that each substituted Nb^{5+} ion polarizes a cluster in the $KTaO_3$ host lattice of some 100 Å^3.

Recently, hyper-Rayleigh data in nominally pure $KTaO_3$ were discussed in terms of impurity-induced clusters.[8] These clusters may lead to a strong central component in the Raman spectra of $KTa_{1-x}Nb_xO_3$ (Ref. 6) and to a pressure-induced dispersion in the low-frequency dielectric constant.[9]

This raises the main open question in $BaTiO_3$ and in all ABO_3 perovskites: Are the local distortions in the cubic phase an intrinsic mechanism or do unwanted impurities have to be invocated in order to account for the nondisplacive behavior near T_c?

A complete understanding of the phase transition requires a complete knowledge of the microscopic interaction within the lattice. Any local distortion in ABO_3 induces an electric dipole moment leading to local polar clusters. The long-range electric dipolar interaction among these polar clusters has to be included in any model. High-frequency (10^6 Hz $< f < 10^9$ Hz) dielectric experiments were performed to probe the dipolar dynamics in $SrTiO_3$,[10] in Ca-doped $SrTiO_3$,[11] in pure and doped $KTaO_3$,[10] and in pure and Fe-doped $BaTiO_3$.[12] Although a quantitative agreement between different techniques is hardly achieved,[7,8,9] the observed monodispersive dielectric relaxation could fit with all the experimental results already mentioned. Moreover, the analysis of dielectric dispersion data is useful to clearly distinguish between individual localized relaxation and random correlation between these local motions.[13] In this paper, we report dielectric dispersion experiments in single crystals of $BaTiO_3$ doped with niobium. The substituted heterovalent ions may be understood as local probes for the lattice relaxation-made dynamics. More precisely, we have evidenced a link between the dc conductivity σ and the dielectric relaxation parameters. The lattice polar clusters of $BaTiO_3$ interact with the Nb-induced conducting electrons. The resulting dipolar moment is 20 times higher in $BaTiO_3$:Nb than in $BaTiO_3$ at all temperatures. At low temperatures $T < 180$ K, a maximum in the dc conductivity is followed by a slowing down of the dielectric relaxation.

In Sec. II we shall describe the sample preparation and the experimental procedure. In Sec. III, we shall report the observed dielectric dispersion in low-doped and

high-doped $BaTiO_3$ single crystals. In Sec. IV we discuss the link between the conductivity and the relaxation in $BaTiO_3$:Nb and we try to describe the interaction between the conduction electrons and the lattice polar clusters.

II. CRYSTAL PREPARATION AND EXPERIMENTS

Doping ceramics of $BaTiO_3$ with Nb impurities leads to semiconducting properties which are used for application purposes. However, in this case, the grain boundaries are not well defined, and this precludes a complete description of electrical measurements. That is why we actually use single crystals of Nb-doped $BaTiO_3$.

Niobium-doped $BaTiO_3$ single crystals were grown in our laboratory using the top-seeded solution growth (TSSG) pulling method. In the investigated crystals, the Nb concentration was 0.1, 0.2, and 0.3 at. %.

The semiconducting behavior of these crystals was probed previously by dc conductivity and light absorption.[14] The enhanced conductivity by 5 orders of magnitude was ascribed to the substitution of Ti^{4+} by Nb^{5+} at the center of the oxygen cage. Computer simulations were performed to find the energy levels introduced in the gap of $BaTiO_3$.[14]

In this study we used the same crystals as the one tested in dc conductivity measurements. The samples were cut in small $3\times3\times1$ mm^3 slits with their major faces parallel to the (100) crystallographic plane. In order to avoid any surface effect in our dielectric results, we performed a careful polishing with diamond paste and etching in orthophosphoric acid for 10 min at 150 °C. This chemical treatment is necessary to remove the surface layer induced during the mechanical polishing. Two opposite faces of the samples were electroded by gold vapor deposition. We noted that gold or palladium sputtering may result in a strong metal clustering at the surface. In such cases, scanning electron microscopy revealed a discontinuous metal surface, and anomalous high-frequency dielectric dispersion was observed.[15] Accordingly, we have not used sputtered electrodes.

All the electrical connections from the samples to the impedance setup were achieved through direct metal-metal contact. Silver paste was used at low frequencies only for mechanical purposes. The experimental setup is based on two Hewlett Packard impedance analyzers: HP 4192 ($5\ \text{Hz} < f < 10^7$ Hz) and HP 4191 ($10^6\ \text{Hz} < f < 10^9$ Hz).[16]

The sample temperature was monitored from 4 to 450 K using standard Dewars and oven. To prevent any residual domain-wall effect in the cubic phase the experimental procedure was the following: The samples were annealed at 400 K, and the dielectric dispersion was recorded at fixed temperatures during the cooling.

III. RESULTS

We first recall the main results obtained in pure and Fe-doped $BaTiO_3$ already published in Ref. 12. In these samples, the high-frequency dielectric dispersion is restricted to high frequencies (Fig. 1, right-hand side). The dielectric anomaly in both the real part $\epsilon_1(\omega)$ and the imaginary part $\epsilon_2(\omega)$ of the dielectric susceptibility is well fitted by a monodispersive Debye relaxation law

$$\epsilon^*(\omega)=\epsilon_1(\omega)-j\epsilon_2(\omega)=\epsilon_\infty+(\epsilon_S-\epsilon_\infty)/(1+j\omega\tau)\ , \qquad (1)$$

where ϵ_∞ stands for the dielectric susceptibility, $\epsilon_1(\omega)$ for frequencies above the dispersion step, $\epsilon_S-\epsilon_\infty$ is the relaxation step, and τ the relaxation time. We attempted to fit the data with a distribution of relaxation times, but the distribution width was never significant so that in the following we will discuss the fits using Eq. (1). The temperature variation of the fitting parameters is as follows: $\epsilon_S-\epsilon_\infty$ is maximum at the cubic-to-tetragonal transition temperature $T_c\sim130$ °C: $\epsilon_S-\epsilon_\infty(T_c)\approx6000$; the relaxation time τ is maximum at T_c, $\tau(T_c)\approx10^{-7}$ s; these anomalies are restricted to a narrow temperature range around T_c. Smoother anomalies in $\epsilon_S-\epsilon_\infty$ and in τ are seen at the tetragonal-to-orthorhombic transition ($T\sim280$ K) and at the orthorhombic to rhombohedral transition ($T\sim-90$ °C or 180 K). When the temperature is not close to one of the three ferroelectric transition temperatures and when the frequency is at least 1 order

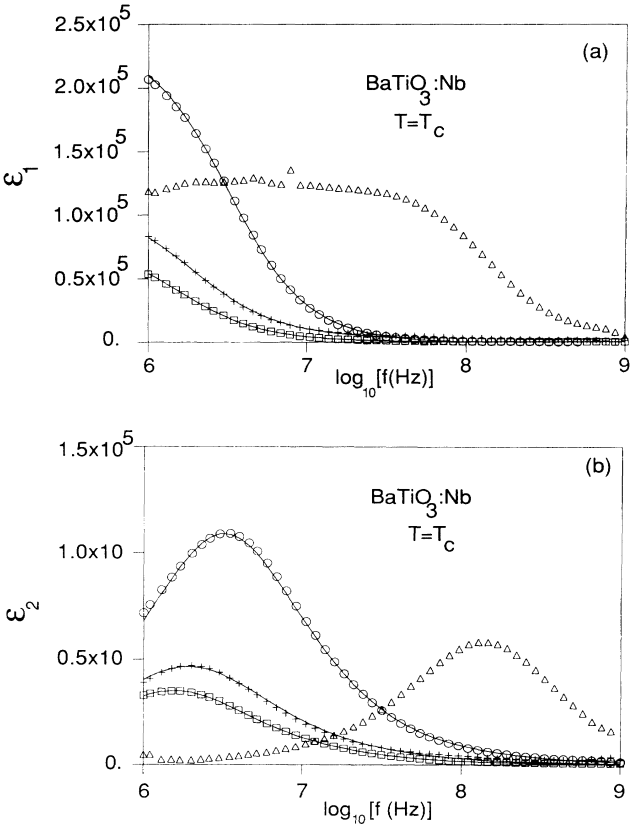

FIG. 1. Dielectric dispersion in the radio frequency range in Nb-doped $BaTiO_3$. (a) The real part is ϵ_1, (b) the imaginary part ϵ_2. The niobium concentration is 0 at. % (triangles), 0.1 at. % (squares), 0.2 at. % (crosses), and 0.3 at. % (circles). The 0 at. % data were multiplied by 20 (see Ref. 12). All these data were recorded at T_c the cubic-to-tetragonal transition temperature, following the thermal treatment described in the text. The lines are the results of least-squares-fits using Eq. (1).

of magnitude away from the relaxation frequency $(2\pi/\tau)$, the dynamic conductivity $\epsilon_2(T,f)$ is nearly zero. This shows that the only contribution to the dielectric losses in pure and slightly Fe-doped $BaTiO_3$ is due to dipolar motion within the lattice.

When the Nb concentration is raised up to 0.1–0.3 %, the conductivity of $BaTiO_3$:Nb shifts from a pure p-type semiconductor to an n-type semiconductor.[14] The static conductivity σ related to this semiconducting behavior may be introduced into the dispersion equation (1)

$$\epsilon^*(\omega)=\epsilon_1(\omega)-j\epsilon_2(\omega)=\epsilon_\infty+\frac{\epsilon_S-\epsilon_\infty}{1+j\omega\tau}-j\frac{\sigma}{\omega} . \quad (2)$$

Equation (2) means that at low frequencies a $1/\omega$ contribution has to be detected in $\epsilon_2(\omega)$, while no extra dispersion occurs in $\epsilon_1(\omega)$. At room temperature, these low-frequency losses do not appear in our frequency range (10 Hz $< f < 10^9$ Hz); the static conductivity σ is too low and the σ/ω term is canceled in Eq. (2). Later on, we will see that this is not true for all temperatures.

More unusual is the value of the static susceptibility $\epsilon_S=\epsilon_1(f)$ for $f < 10^4$ Hz. At all temperatures, ϵ_S is more than 20 times higher than in pure and slightly doped $BaTiO_3$.

This high static susceptibility was already measured in one sample of $BaTiO_3$:Nb.[17] In the present study, we show that $\epsilon_S(BaTiO_3{:}Nb)$ is greater than $\epsilon_S(BaTiO_3)$ for all the investigated samples. Near T_c, the cubic-to-tetragonal transition temperature, the ratio $\epsilon_S(BaTiO_3{:}Nb/\epsilon_S(BaTiO_3)$ increases from 10 to 20 when the Nb content is raised from 0.1 to 0.3 at. % (Fig. 1). Moreover, the extended temperature and frequency ranges that we have used allow a comparison of the dielectric relaxation in $BaTiO_3$:Nb and in $BaTiO_3$.

In the cubic phase, the dielectric relaxation in $BaTiO_3$:Nb (0.1–0.3 at. %) occurs at frequencies much lower than in pure $BaTiO_3$ (Fig. 1, left-hand side): 5×10^6 Hz instead of 10^8 Hz at T_c+1 °C. This decrease by 1 order of magnitude was never observed in $BaTiO_3$ samples doped with Fe, Co, or Li. Since the dielectric relaxation in $BaTiO_3$:Nb is monodispersive, we could fit the data with Eq. (1). The most striking result that we actually report concerns the temperature variation of this dielectric dispersion. Figure 2 displays the temperature variation of $\epsilon_S-\epsilon_\infty$ and τ^{-1}. While for pure $BaTiO_3$ the relaxation rate τ^{-1} is always faster than 10^8 s^{-1}, τ^{-1} drops down below $T\sim180$ K in $BaTiO_3$:Nb 0.1 and 0.3 at. %. At temperatures lower than 30 K, the relaxation is below our lowest frequency $f\sim10$ Hz. In Fig. 3, we tried an Arrhenius description of this slowing down. The Arrhenius law $\tau=\tau_0\exp(E/K_BT)$ holds for $BaTiO_3$:Nb 0.1 and 0.3 at. % below 180 K. The Arrhenius parameters are calculated using a linear regression of the points of Fig. 3 (Table I). The activation energy E and basic relaxation time τ_0 are nearly the same for the three $BaTiO_3$:Nb samples. The basic relaxation frequency $f_0\approx10^8$ Hz is much lower than usual ionic frequencies $f_0\approx10^{13}$ Hz; this confirms that the relaxation is not a single-ion process.

In the same temperature range the relaxation strength $\epsilon_S-\epsilon_\infty$ is nearly temperature independent [Fig. 2(a)]. This is rather unusual because, in classical dipolar relaxa-

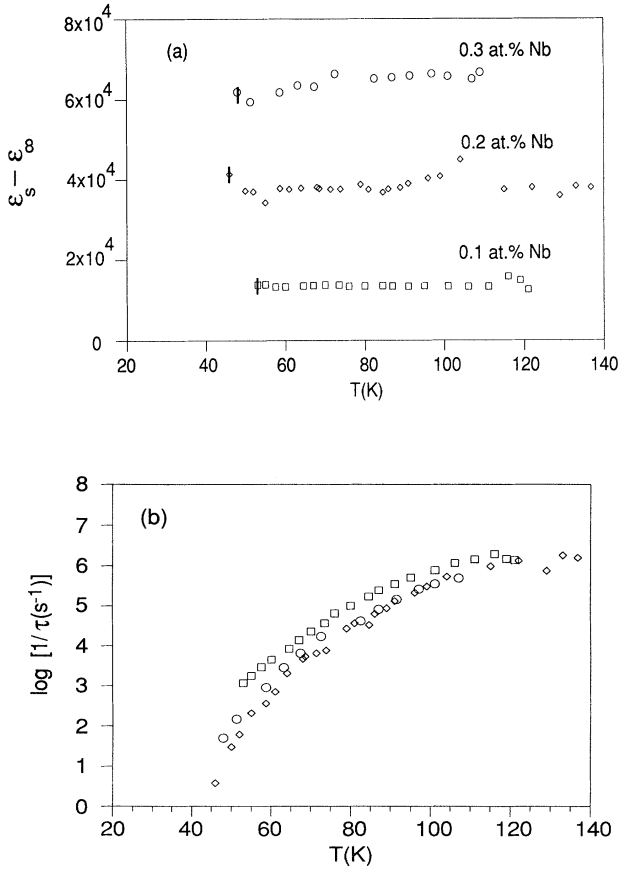

FIG. 2. (a) Relaxation step $\epsilon_S-\epsilon_\infty$ vs temperature for $BaTiO_3$:Nb in the rhombohedral phase, $T<180$ K. The fitting error is sketched by the vertical bars. (b) Logarithm of the inverse relaxation time vs temperature in the rhombohedral phase of $BaTiO_3$:Nb. At higher temperatures, from 180 up to 430 K, the inverse relaxation time is always between 10^6 and 10^7 s^{-1}. For pure and Fe-doped $BaTiO_3$, the inverse relaxation time stays always above 10^8 s^{-1} (see Ref. 12).

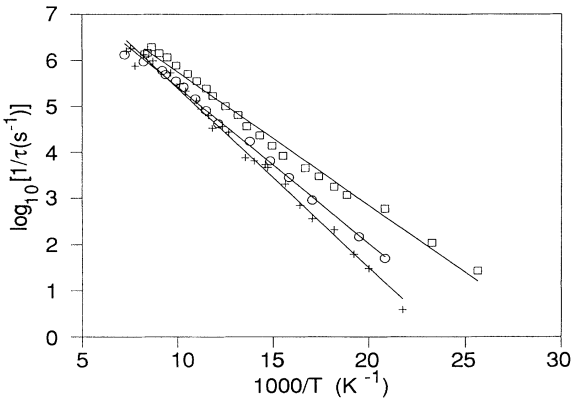

FIG. 3. Arrhenius plot of the relaxation rate in $BaTiO_3$:Nb in the rhombohedral phase. The lines stand for a linear regression of the data to the Arrhenius law. The activation energies E and basic relaxation rates are given in Table I.

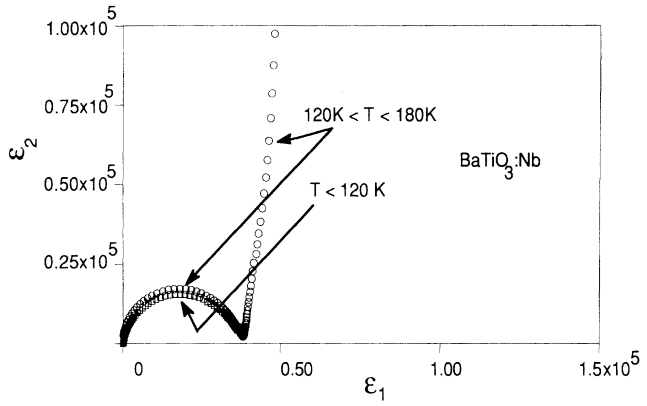

FIG. 4. Cole-Cole plot of the dielectric dispersion in $BaTiO_3$:Nb, 0.1–0.3 at. % Nb. The data for $120 < T < 180$ K are described by Eq. (2) and the data for $T < 120$ K by Eq. (1).

tion, any slowing down of a relaxation is connected with an increase of the relaxation strength. We will come back to this point in the discussion.

At last we focus on the precursor effect of this slowing down. At the third ferroelectric phase transition $T \sim 180$ K, there is a large maximum in the dc conductivity. This is obvious in Fig. 4 where we have plotted $\epsilon_2(\omega)$ versus $\epsilon_1(\omega)$ for temperatures around 180 K. The left-hand side semicircle is nothing but the dielectric relaxation already described. The right-hand side is nearly a vertical line: $\epsilon_2(\omega)$ increases and $\epsilon_1(\omega)$ is constant when ω decreases. This means that Eq. (2) holds for the dielectric dispersion in this temperature range.

In Fig. 5, we have plotted the low-frequency ($f < 100$ Hz) imaginary part of the dielectric susceptibility which is sensitive to the dc conductivity. This dc conductivity σ increases sharply at the orthorhombic-to-rhombohedral phase transition ($T = 180$ K). Below this temperature, there is a rounded maximum in σ and, at 90 K, the high-temperature value of σ is recovered.

A complete description of Fig. 5 leads to the very

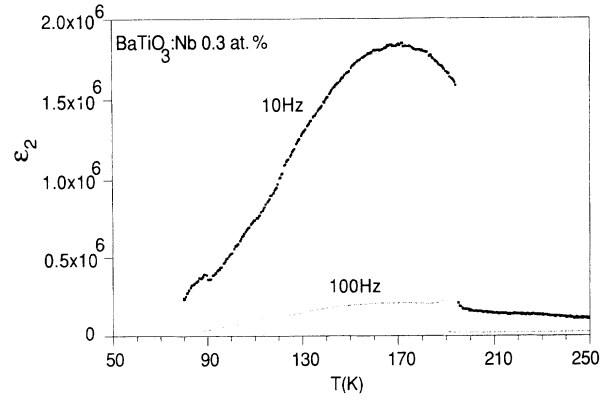

FIG. 5. Low-frequency conductivity of $BaTiO_3$ 0.3 at. % Nb. The broad maximum in $\epsilon_2(T)$ for frequencies lower than 100 Hz results from the σ_{dc}/ω term in Eq. (2) for temperatures between 120 and 180 K.

TABLE I. Arrhenius parameters of the low-temperature slowing down of the relaxation motion in $BaTiO_3$:Nb.

Sample (at. % Nb)	Activation energy E (eV)	Basic relaxation time τ_0 (s)	Basic relaxation frequency f_0 (Hz)
0.1	3.3×10^{-2}	5.3×10^{-10}	3×10^{8}
0.2	2.5×10^{-2}	2.5×10^{-9}	6.3×10^{7}
0.3	3×10^{-2}	1×10^{-9}	1.4×10^{8}

specific features of the dielectric relaxation in the rhombohedral phase of $BaTiO_3$:Nb. First, the orthorhombic-to-rhombohedral transition is followed by an increase of the static conductivity. Just below the conductivity maximum, the dielectric relaxation starts to slow down while the relaxation strength remains constant.

IV. DISCUSSION

A model for the dielectric relaxation in $BaTiO_3$:Nb has to account for the very high relaxation step and to describe—at least qualitatively—the slowing down of this relaxation motion in the rhombohedral phase. At any temperature, the relaxation step $\epsilon_S - \epsilon_\infty$ in $BaTiO_3$:Nb is 25 times higher than in pure and Fe-doped $BaTiO_3$.

In a simple Langevin model, the relaxation step is related to the local relaxing units p:

$$\epsilon_S - \epsilon_\infty = \frac{Np^2}{3k_B T \epsilon_0} , \tag{3}$$

where N is the density of dipoles p. In pure $BaTiO_3$, p is ascribed to off-center Ti^{4+} ions. To understand the whole dispersion step in pure and Fe-doped $BaTiO_3$, dynamical correlations between these individual Ti^{4+} ions were introduced.[12] The correlation volume was some 4000 Å^3 at 400 K, in rough agreement with diffuse x-ray data.[2] In the following, we will call this dynamical correlation between off-center Ti^{4+} ions "clustering."

The relaxation time τ of the dielectric relaxation is related to the local multiwell potential in which the dipoles are moving. In the case of pure and Fe-doped $BaTiO_3$, the off-center Ti^{4+} ions move in an eight-well potential at the center of the oxygen cage. τ may be related to the barrier height E between these wells.

The results reported here for $BaTiO_3$:Nb do not fit in this picture. First of all, the huge dispersion step $\epsilon_S - \epsilon_\infty \sim 200\,00$ in $BaTiO_3$:Nb 0.3 at. % cannot be understood in the framework of the dynamic clustering of off-centered Ti^{4+} ions. This would require clusters of size 80 000 Å^3 and percolation between these extended clusters would preclude any Debye-like relaxation. The slowing down of the relaxation motion below 180 K is not due to direct dipolar interaction between Nb^{5+} impurities and Ti^{4+} relaxation modes. In such a case, randomly distributed impurities lead to random dipolar interaction.[13] This enhances the distribution of activation energies and thus the distribution of relaxation times probed in our experiment. In all the investigated samples, this distribu-

tion of relaxation times was always negligible (Figs. 1 and 3). Moreover, domain or domain-wall dynamics are not the key mechanism for this relaxation. If so, pure, Fe-doped, and Nb-doped $BaTiO_3$ would behave in the same way. This is not observed. In pure and Fe-doped $BaTiO_3$ the relaxation frequency is always higher than 10^7 Hz. In $BaTiO_3$:Nb, the relaxation frequency is always lower than this value.

The dielectric relaxation in $BaTiO_3$:Nb is neither a pure ionic effect nor a domain motion. Up to now, the main contribution of Nb^{5+} impurities in the dielectric properties of $BaTiO_3$:Nb was the electronic conductivity $\sigma \sim 10^{-4}\ \Omega^{-1}\,cm^{-1}$ instead of $\sigma \sim 10^{-10}\ \Omega^{-1}\,cm^{-1}$ in pure $BaTiO_3$.[14]

Any ionic motion within the host lattice has to interact with these conducting electrons. An electron–relaxation-mode model may explain the anomalous dielectric dispersion in $BaTiO_3$:Nb. The high-dispersion step $\epsilon_S - \epsilon_\infty \sim 200\,000$ is understood if each of the lattice relaxation modes is enhanced by an electronic charge of 5. In fact, the pure lattice relaxation step is $\epsilon_S - \epsilon_\infty \sim 8000$ at 400 K, the cubic-to-tetragonal transition temperature; using Eq. (3) and multiplying p by 5 increases $\epsilon_S - \epsilon_\infty$ by 25. Recalling that the polar cluster volume is some 4000 $Å^3$ in pure $BaTiO_3$, only a limited number of conducting electrons has to contribute to the effective charge of the relaxation mode in $BaTiO_3$:Nb. In this picture, the conduction electrons do not screen the lattice polar cluster. The electrons may increase the effective polar moment if they are trapped on impurity levels within the polar clusters. Obviously, dielectric spectroscopy cannot resolve such local valency effects, and further experimental work is needed.

Moreover, monodispersion is conserved because the correlation length of each polar cluster does not increase when lowering the temperature. This also explains why $\epsilon_S - \epsilon_\infty$ does not diverge when the relaxation slows down. In our view, the low-temperature slowing down also results from an interaction with the conducting electrons.

The conductivity mechanism in $BaTiO_3$:Nb has been much discussed in the literature[18] on the basis of experiments performed on ceramics. Obviously, the grain boundary conductivity is the main unknown parameter. It seems, however, that the bulk n-type conductivity of the grains is related to a thermally activated motion of a particle, being a polaron[19] or an electron. The conductivity results from particle hopping between the impurities whose ionicity may change from site to site. For example, the ionic charge of niobium may be 5+ or 4+ and the ionic charge of oxygen vacancies may be 2+ or 1+. Using such a simplified model, one cannot explain the abrupt increase of σ at the orthorhombic-to-rhombohedral phase transition (Fig. 5). In fact, a sudden change of the ionic charge of the impurities is rather unlikely at a phase transition where only the mean crystal symmetry is transformed. We, however, ascribe the subsequent decrease of σ at $T < 120$ K to the relocalization of electrons on their impurity levels. Such a redistribution of conducting electrons induces a redistribution of the ionic charges of impurities located outside the polar clusters. As a consequence, the local potential around each relaxing unit p is changed through Coulomb interaction. In this process, the slowing down of the relaxation motion is related to the thermally activated relocalization of electrons. We note that the activation energies given in Table I are in agreement with the well-known activation energy of electrons on oxygen vacancy levels:[18] 0.05 eV. Recent polaronic models[20] also gave nearly the same activation energy (0.06 eV).

Our model also explains why the relaxation motion slows down while the relaxation strength $\epsilon_S - \epsilon_\infty$ stays constant. It is only the local potential which sharpens when T decreases below 120 K. The effective dipole moment does not change either by an increase of the cluster size or by an increase of the dipole charge. This last statement is confirmed by the Arrhenius parameters given in Table I. The basic relaxation frequency $f_0 \approx 10^8$ Hz is roughly the same as the relaxation frequency of the lattice clusters.

Thus, in this model, we postulate that the electron lattice interaction is restricted to an electron–relaxation-mode one. Moreover, it is not the relaxation motion which influences the conduction but rather the conducting electrons which increase the dipole moment at all temperatures and increase the multiwell barrier height in the rhombohedral phase.

In this sense, we consider exactly the reverse of classical polaronic models. The polaronic conduction, e.g., in $BaTiO_3$:Fe arises from phonon-assisted hopping of holes.[19] Ionic vibrations within the lattice increase the impurity-induced conductivity. In the electron–relaxation-mode model that we propose here, the impurity-induced conductivity interacts with the main contribution to the dielectric susceptibility: the relaxation mode.

V. CONCLUSION

We tried to summarize our experimental findings in Fig. 6. The intrinsic relaxation mode in nominally pure $BaTiO_3$ was ascribed to polarized clusters of off-center Ti^{4+} ions[12] [Fig. 6(a)]. In $BaTiO_3$:Nb, the electronic contribution to this relaxation-mode dynamics is twofold. First, at all temperatures, the free electrons within each cluster may be nonrandomly distributed [Fig. 6(b)]. This increases the local dipole moment of each local cluster. This effect is probably due to the substitution of Ti^{4+} ions by Nb^{5+} ions. In the rhombohedral phase of $BaTiO_3$:Nb ($T < 180$ K), the free electrons outside the clusters localize on impurity levels such as Nb^{5+}, Nb^{4+}, $VO\cdot\cdot$, $VO\cdot$. This is the only way to avoid the screening of the local relaxation mode by the electrons. This electron localization outside the clusters increases the barrier height of the multiwell local potential around each relaxing unit (Fig. 6(c)]. As a consequence, the relaxation motion slows down while the relaxation step stays constant. We stress that this tentative model has to be tested and improved. Dielectric spectroscopy is not able to resolve the local valency changes following the electron localization. The only indirect signature of this electron trapping is

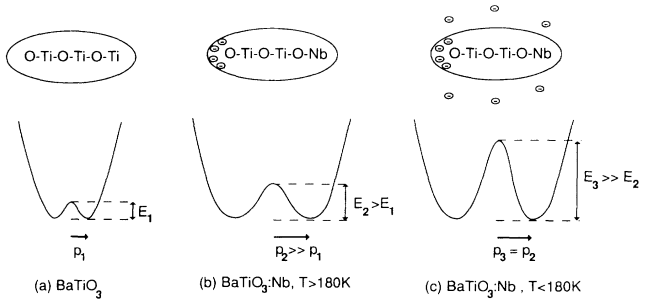

FIG. 6. Schematic drawing of the electron–relaxation-mode interaction in $BaTiO_3$:Nb. Upper part: the relaxing clusters where the minus sign stands for the electronic charge. Lower part: a one-dimensional sketch of the multiwell potential in which the clusters relax. In nominally pure $BaTiO_3$, the relaxation mode is described by an effective dipole moment p_1 and an interwell barrier height E_1 (a). In $BaTiO_3$:Nb, the electron distribution within a cluster increases strongly the dipole moment and slightly the barrier height (b). The low-temperature electron localization outside the clusters increases the barrier height (c).

the slowing down of the relaxation motion (Fig. 3).

Nevertheless, we think that, in some cases, the classical polaron model for the conductivity in doped $BaTiO_3$ has to be reconsidered. Instead of a pure electron-phonon interaction, an electron–relaxation-mode mutual interaction may be the key for a complete description of the conductivity enhancement in *n*-type $BaTiO_3$. Moreover, since for $T > 180$ K the temperature variation of the relaxation parameters in $BaTiO_3$:Nb and in $BaTiO_3$ are not qualitatively different, our dielectric results are in favor of an impurity-induced relaxation mode. In the case of nominally pure samples, the "unwanted" impurities can be oxygen vacancies. Even if this conclusion is in agreement with theoretical predictions,[21] we think that we have not given a clear answer to this question. Recently, a relaxational dynamics was deduced from lattice dynamics computations applied to $BaTiO_3$.[22]

Finally, our observation of an electron localization may be of some use for other investigations. In light-scattering experiments, a dressed relaxation mode may be included to model the strong central lines even in the case of nominally pure $BaTiO_3$ and $KNbO_3$. This could eventually help in understanding the failure of the Lyddane-Sachs-Teller equation in these perovskites.

ACKNOWLEDGMENTS

It is our pleasure to acknowledge continuous stimulating discussions with U. T. Hochli, M. Fontana, B. Jannot, and technical assistance by A. Gueldry and P. Lompre. This work was partially supported by the "Ministère de la Recherche et de la Technologie." Laboratoire de Physique du Solide is Unité Associeé No. 785 du Centre National de la Recherche Scientifique.

[1]W. Cochran, Adv. Phys. **10**, 401 (1961).
[2]R. Comes, M. Lambert, and A. Guinier, Solid State Commun. **6**, 715 (1968).
[3]K. A. Muller, Y. Luspin, J. L. Servoin, and F. Gervais, J. Phys. (Paris) Lett. **43**, 537 (1982).
[4]G. Burns and B. A. Scott, Solid State Commun. **13**, 417 (1973).
[5]M. D. Fontana and G. E. Kugel, Jpn. J. Appl. Phys. **24**, Suppl. 24-2, 223 (1985); H. Uwe, K. B. Lyons, H. L. Carter, and P. A. Fleury, Phys. Rev. B **33**, 6436 (1986).
[6]K. A. Muller, W. Berlinguer, K. W. Blazey, and J. Albers, Solid State Commun. **61**, 21 (1985).
[7]J. J. van der Klink, S. Rod, and A. Chatelain, Phys. Rev. B **33**, 2048 (1986).
[8]H. Vogt, Phys. Rev. B **41**, 1184 (1990).
[9]G. A. Samara, Phys. Rev. Lett. **53**, 298 (1984).
[10]M. Maglione, S. Rod, and U. T. Höchli, Europhys. Lett. **4**, 631 (1987).
[11]W. Kleeman and H. Schremmer, Phys. Rev. B **40**, 7428 (1989).
[12]M. Maglione, R. Böhmer, A. Loidl, and U. T. Höchli, Phys. Rev. B **40**, 11 441 (1989).
[13]U. T. Höchli, Phys. Rev. Lett. **48**, 1494 (1982).
[14]P. Moretti, G. Godefroy, and J. M. Bilbault, Ferroelectrics **37**, 721 (1981).
[15]M. Belkaoumi and M. Maglione (unpublished).
[16]R. Böhmer, M. Maglione, P. Lunkenheimer, and A. Loidl, J. Appl. Phys. **65**, 901 (1989).
[17]G. Godefroy and A. Perrot, Ferroelectrics **54**, 87 (1984).
[18]H. Ihrig and D. Hennings, Phys. Rev. B **17**, 4593 (1978).
[19]A. Zylberstein, Appl. Phys. Lett. **29**, 778 (1976).
[20]G. Chanussot, Ferroelectrics **115**, 49 (1991).
[21]A. P. Levanyuk (private communication).
[22]R. E. Cohen and H. Krakauer Phys. Rev. B **42**, 6418 (1990).